ELSEVIER

Journal of Arid Environments 72 (2008) 1329–1342

Journal of Arid Environments

www.elsevier.com/locate/jaridenv

Regional maximum wind speed frequency analysis for the arid and semi-arid regions of Iran

R. Modarres*

Faculty of Natural Resources, Isfahan University of Technology, Isfahan, Iran

Received 30 July 2006; received in revised form 16 December 2007; accepted 20 December 2007
Available online 20 February 2008

Abstract

Although many papers have been published on the role of wind speed on wind erosion, most of them did not consider the probability or return period of wind speed and its role in wind erosion. This study deals with this characteristic of wind speed in arid and semi-arid regions of Iran. Because at-site frequency analysis is not sufficient for extending wind frequency to locations with no data, the method of L-moments was applied for regional frequency analysis. The results of this study showed the Generalized Logistic (GLOG) distribution model to be the best regional distribution model for 3-h maximum mean annual wind speeds within homogeneous region based on goodness-of-fit test measurement, Z^{Dist}. The extension of different wind quantiles to the region showed that the center, southwestern and northwestern parts of the study area could be more vulnerable regions to wind erosion than other parts. The comparison of wind energy for different wind speed return periods indicates a nonlinear trend in wind energy when the return periods increase. Therefore, it is important to apply wind frequency analysis in wind erosion control projects because the risk of higher wind speed does not increase with linear function.

Keywords: Arid region; GLOG distribution model; Iran; L-moments; Maximum wind speed; Regional frequency analysis; Wind energy; Wind erosion

1. Introduction

Wind is the major environmental phenomenon in arid and semi-arid regions of the world and wind erosion is a major environmental and agricultural world problem, which has intensified in recent years. Because of their climate, arid and semi-arid regions of the world are the principal domain of wind erosion (Gomes et al., 2003).

Dry surface and sparse vegetation in these regions cause potential environmental condition for wind erosion and aeolian processes. Scientists agree that land use change, usually from rangelands to cultivated fields, in these regions significantly increase wind erosion activity (Stout and Lee, 2003). Wind erosion not only results in destruction of soil structure, but also affects land production potential (Lopez, 1998). Wind erosion is also considered to be the principal mechanism of land degradation (Okin et al., 2001), dust storm generation and its health impacts (Song, 2004; Zobeck and van Pelt, 2006).

*Tel.: +98 3112675601.
E-mail address: r_m5005@yahoo.com

0140-1963/$ - see front matter © 2007 Elsevier Ltd. All rights reserved.
doi:10.1016/j.jaridenv.2007.12.010

During recent decades, the destruction of vegetation by intensive grazing and increasing abandoned farmlands and soil erosion has resulted in frequent sand storms, sand dune invasion and substantial socioeconomic problem in arid and semi-arid regions of Iran. Although wind erosion is a complex phenomenon, which is influenced by different factors such as terrain conditions, climatic factors and human management (WEPS, 1996), wind speed has a main role in wind erosion and its intensity. The driving force of wind, which causes the movement of soil particles, has significant relationship with wind speed. Another important characteristic related to wind speed is frequency and direction. In this study, we focus only on wind speed frequency. A glance at a frequency versus wind speed histogram is not sufficient for frequency analysis. Wind speed frequency analysis is an essential task for risk analysis related to any wind erosion control project during its design life, such as wind breaks (Cornelis and Gabriels, 2005). For example, what is the probability of the occurrence of a wind speed greater than a threshold speed (i.e. 40 m/s) for a wind-break project during its design life (i.e. next 10 years)? In this case, another problem will come up. At site, frequency analysis is not enough because a manager or wind erosion structure designer usually needs wind frequency analysis where no data or no wind speed measurement is available. Here, we need to use methods, which extend the results of at-site frequency analysis to a wide region. This extension is usually called ''pooled frequency analysis'' or ''regional frequency analysis''. In this paper, we use regional frequency analysis to extend at-site 3-h maximum mean annual wind speed frequency analysis of 19 wind stations to the arid and semi-arid regions of Iran.

2. Regional frequency analysis

The term pooled frequency analysis was first given to regional frequency analysis by Reed et al. (1999). In the recent literature, the term ''regional'' has been replaced by the term ''pooled'' as the regions, used in typical regional frequency analysis, are no longer fixed and geographically contiguous (Goel et al., 2004). This approach can be applied to sites that are either unmeasured or have a wind record that is not long enough to afford an accurate estimate of the quantile of interest. The approach involves the following steps:

(i) formation of pooling groups (homogeneous regions),
(ii) checking the regional homogeneity of the group,
(iii) identification of the regional distribution function for the groups and estimation of its parameters.

In recent years, the method of L-moments, introduced by Hosking (1990), has been widely used for regional frequency analysis in the fields of atmospheric and hydrologic analysis since then. In the following sections, the method of L-moments and their related statistics used for forming pooling groups are described.

2.1. L-moments

L-moments are modifications of the probability weighted moments (PWMs) introduced by Greenwood et al. (1979) and are linear combinations of PWMs The estimators of L-moments are relatively insensitive to outliers (Vogel and Fennessey, 1993). The mathematical formulation of L-moments using PWMs is briefly presented here. Hosking and Wallis (1993) present the following relationships:

$$\lambda_1 = \beta_0, \tag{1}$$

$$\lambda_2 = 2\beta_1 - \beta_0, \tag{2}$$

$$\lambda_3 = 6\beta_2 - 6\beta_1 + \beta_0, \tag{3}$$

$$\lambda_4 = 20\beta_3 - 30\beta_2 + 12\beta_1 - \beta_0, \tag{4}$$

where λ_r are L-moments and β_r are PWMs defined as

$$\beta_r = \int_0^1 x(F)F^r \, \mathrm{d}F, \tag{5}$$

where F is the non-exceedence probability.

L-moments are directly interpretable as measures of the scale and shape of probability distribution models. Clearly, λ_1, the mean, is a measure of location. λ_2 is a measure of scale or dispersion of the random variable.

In order to make the L-moments independent of the units of measure of x, it is often convenient to standardize the higher moments as

$$\tau_r = \frac{\lambda_r}{\lambda_2} \quad \text{for } r = 3, 4. \tag{6}$$

Analogous to the conventional moment ratio, such as the coefficient of variation, the L-coefficient of variation, LCv, is defined as

$$\mathrm{LCv} = \frac{\lambda_2}{\lambda_1}. \tag{7}$$

The corresponding L-coefficient of skewness (LCs) reflects the degree of symmetry of a sample. It has limits $-1 < \mathrm{LCs} < 1$; symmetric distribution models have LCs = 0. Similarly, LCk is a measure of peakedness and is referred to as the L-coefficient of kurtosis.

2.2. Formation of homogeneous regions

This approach involves forming a set of stations, called pooled groups. The members of the group are considered to be similar in some attributes.

In the formation of a pooling group, all sites that have a high similarity with the site of interest are grouped together. A number of similarity measures, based on Euclidean distance computed in a multidimensional attribute space, have been proposed in the literature (see e.g. Cunderlik and Burn, 2002; Reed et al., 1999). In the present work, the pooling groups for the wind measuring stations in the arid region of Iran are formed based on the method of L-moments (Hosking and Wallis, 1993).

Three statistical measures are used to form a homogeneous region, (i) discordancy measure, (ii) heterogeneity measure and (iii) goodness-of-fit measure (Hosking and Wallis, 1993) The next section of the paper describes these three statistical measures.

2.3. Discordancy measure

The discordancy measure, D_i, is used to find out unusual sites from the pooling group (i.e., the sites whose at-site sample L-moments are markedly different from the other sites). D_i is defined as follows:

$$D_i = \tfrac{1}{3}(u_i - \bar{u})^{\mathrm{T}} S^{-1} (u_i - \bar{u}), \tag{8}$$

where u_i is the vector of L-moments, LCv, LCs and LCk, for a site i:

$$S = (N_{\mathrm{s}} - 1)^{-1} \sum_{i=1}^{N_{\mathrm{s}}} (u_i - \bar{u})(u_i - \bar{u})^{\mathrm{T}}, \tag{9}$$

$$\bar{u} = N_{\mathrm{s}}^{-1} \sum_{i=1}^{N_{\mathrm{s}}} u_i \tag{10}$$

and N_{S} is the number of sites in the group. In general, a site is declared discordant if $D_i > 3$.

2.4. Heterogeneity measure

The heterogeneity measure estimates the degree of heterogeneity in a group of sites and is used to assess whether the group might reasonably be treated as homogeneous. This measure compares the variability of L-moment ratios for the sites in a group with the expected variability, obtained from simulation, for a collection of sites with the same record lengths as those in the group. The statistics used for homogeneity test are three heterogeneity measures (H) namely H_1, H_2 and H_3 with respect to LCv scatter, LCv–LCs and

LCv–LCv, respectively. A region is homogenous if any of H_i is less than 1, possibly heterogeneous if H_i is between 1 and 2, and definitely heterogeneous if H_i is greater than 2 (Hosking and Wallis, 1993).

Hosking and Wallis (1993) observed that the statistics H_2 and H_3 lack the power to discriminate between homogeneous and heterogeneous regions and that H_1 based on LCv had much better discriminating power. Therefore, the H_1 statistic is recommended as a principal indicator of heterogeneity.

2.5. Goodness-of-fit measure

The goodness-of-fit measure is used to identify the regional distribution function for the group. The quality of fit is judged by the difference between the regional average $\bar{t}_4$ and the value of τ_4^{Dist} for the fitted distribution model. The statistic Z^{Dist} for a chosen distribution function is as follows (Hosking and Wallis, 1993):

$$Z^{\mathrm{Dist}} = \frac{\bar{t}_4 - \tau_4^{\mathrm{Dist}}}{\sigma_4}, \tag{11}$$

where $\bar{t}_4$ is the average L-kurtosis value computed from the data of a given region; τ_4^{Dist} the average L-kurtosis value computed from simulation for a fitted distribution model; and σ_4 the standard deviation of L-kurtosis values (from simulation).

A given distribution model is declared a good fit if $|Z^{\mathrm{Dist}}| \leqslant 1.64$. If more than one distribution model meets the above criterion, the preferred distribution model is the one that has the minimum $|Z^{\mathrm{Dist}}|$ value.

3. Study area and data used

3.1. Study area

Arid and semi-arid regions of the Islamic Republic of Iran lie approximately between 44°E and 64°E in longitude and between 25°N and 40°N in latitude. More than 30% of the country provinces are within the arid and semi-arid regions. The region is limited between two main mountain ranges, Elburz and Zagros mountains, in the North and West, respectively. Climatically, like most arid regions, desert-type environment with low annual rainfall of about below 100 mm and dry hot weather characterize the climate of the arid region of Iran.

3.2. Data used

Three-hour maximum mean annual wind speed time series (“maximum wind speed” hereafter) for 19 stations in the arid and semi-arid regions of Iran were selected for this study (Table 1; Fig. 1). For deriving wind data, 3-h wind velocity measurements are averaged and the maximum value of these averaged data is selected for each day. The maximum observed daily value is selected as the annual maximum wind speed. These data are maintained by the Iran Meteorological Organization available at http://www.irimet.net.

The descriptive statistics of the observed annual maximum wind speed of the selected stations are presented in Table 2. The maximum wind speed was observed for Kerman and Boujnord stations, which are in the middle and the north of the arid and semi-arid regions of Iran (Fig. 1). The average annual maximum wind speed for the region is 35 km/h, the average S.D. is 12 km/h and the average coefficient of variation is 32%.

4. Results and discussion

4.1. Moment diagrams

The moment ratio diagram (MRD) is an easy way to identify regional homogeneity of a region. An L-moment diagram provides a visual comparison of sample estimates to population values of L-moments (Stedinger et al., 1993) and are always preferred to product MRDs for goodness-of-fit test (Vogel and Fennessey, 1993). Figs. 2 and 3 show the MRDs of all selected stations for the most important

Table 1
Weather stations with geographical coordinates located in the arid and semi-arid regions of Iran

Stations	Sample size (years)	Latitude (°N)	Longitude (°E)	Altitude (m)
Kashan	37	33°59′	51°27′	982
Boujnurd	26	37°28′	57°19′	1091
Isfahan	53	32°37′	51°40′	1550
Khoor	17	33°47′	55°05′	845
Yazd	51	31°54′	54°24′	1230
Zabol	41	31°02′	61°29′	489
Zahedan	53	29°28′	60°55′	1370
Iranshahr	39	27°12′	60°42′	591
Shahrood	53	36°25′	54°57′	1345
Sabzevar	48	36°12′	57°43′	977
Semnan	38	35°33′	53°23′	1170
Torbat	45	35°16′	59°13′	1450
Tabbas	36	33°36′	56°55′	711
Birjand	45	32°52′	59°12′	1491
Kerman	53	30°15′	56°58′	1753
Shiraz	53	29°36′	52°53′	1488
Bam	44	29°06′	58°21′	1067
Fassa	37	28°58′	53°14′	1288
Chahbahar	34	25°17′	60°37′	08

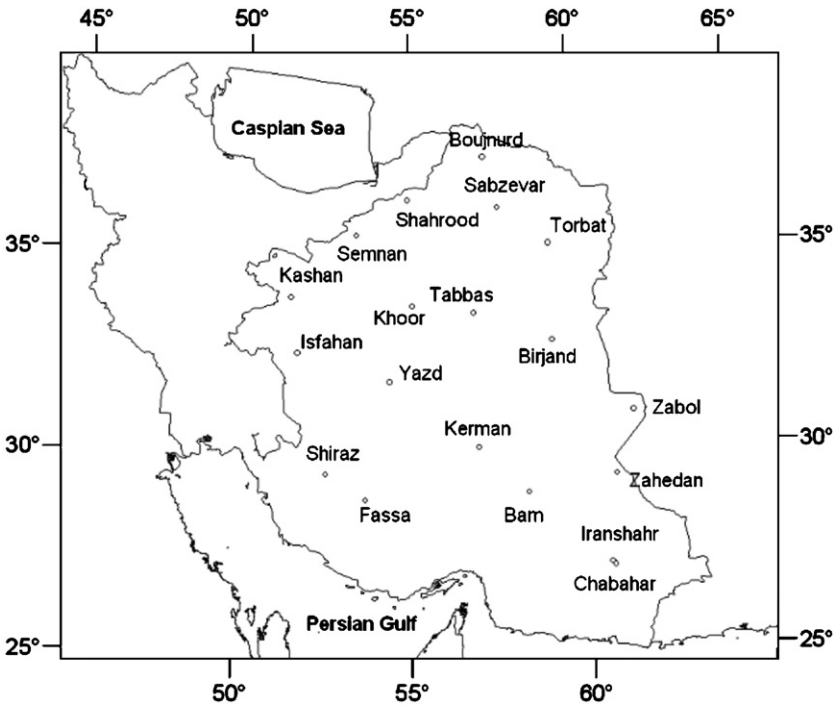

Fig. 1. Spatial distribution of selected stations in arid and semi-arid regions of Iran.

three-parameter distribution models. The L-moments values are also presented in Table 3. The MRD is a graphical method for investigating the regional distribution model but it is not suitable enough to find homogeneous region. Other methods to identify regional homogeneity introduced by Hosking and Wallis (1993) are two statistics discussed in the following section.

Table 2
Statistical characteristics of the annual maximum wind speed in the study area

Stations	Maximum (km/h)	Mean (km/h)	S.D. (km/h)	Coefficient of variation	Skewness	Kurtosis
Bam	74.0	30.9	11.8	0.4	1.8	5.2
Birjand	51.0	30.0	5.6	0.2	1.0	3.1
Boujnord	87.0	49.6	18.0	0.4	0.1	−0.5
Chabahar	40.0	29.1	6.6	0.2	0.1	−0.7
Isfahan	58.0	39.3	6.7	0.2	0.7	0.6
Fassa	54.0	28.2	9.8	0.4	0.6	−0.1
Iranshahr	80.0	36.9	11.0	0.3	1.3	3.3
Kashan	58.0	28.7	9.6	0.3	1.2	1.7
Kerman	97.0	44.4	11.0	0.3	2.3	9.1
Khoor	80.0	53.7	58.7	1.1	4.0	16.5
Sabzevar	45.0	32.7	6.8	0.2	0.2	−1.0
Semnan	50.0	28.5	7.5	0.3	1.0	1.1
Shahrood	50.0	27.3	9.0	0.3	1.0	0.1
Shiraz	58.0	31.1	7.4	0.2	1.1	2.4
Tabbas	58.0	28.5	10.3	0.4	0.9	0.8
Torbat	49.0	28.1	7.5	0.3	0.6	0.1
Yazd	65.0	39.7	8.4	0.2	0.9	0.9
Zabol	80.0	41.9	11.6	0.3	1.4	3.5
Zahedan	80.0	45.1	10.0	0.2	1.2	1.7
Mean	63.9	35.5	12.0	0.3	1.1	2.5

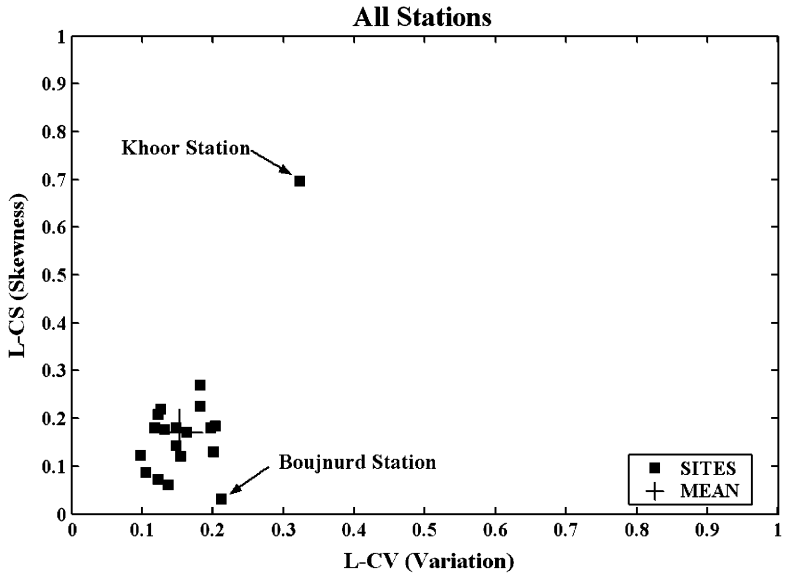

Fig. 2. LCv–LCs moment ratio diagram for 20 wind stations in arid and semi-arid region of Iran.

4.2. Homogeneity and discordancy test

In this section, we first seek the discordant stations by the use of discordancy statistics developed by Hosking and Wallis (1993). The D statistics of the selected stations are presented in Table 3. It can be seen that two stations, Boujnord and Khoor stations have "D" statistics greater than $D = 3$. Khoor station may be anomalous because of the distinctly shorter period of record. Thus these two stations are considered as discordant stations and are removed from the data set. The L-moments of these two stations are also shown in Figs. 2 and 3.

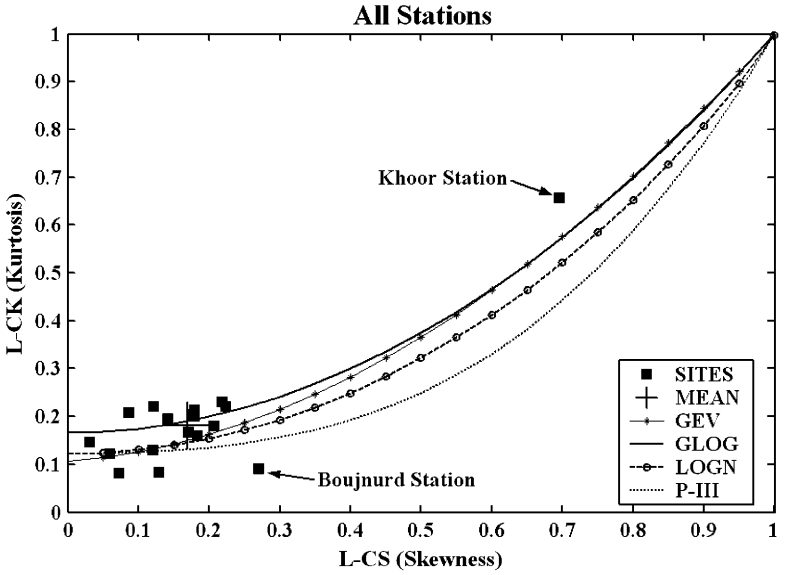

Fig. 3. LCs–LCk moment ratio diagram for 20 wind stations in arid and semi-arid region of Iran.

Table 3
L-moments and discordancy measures for selected stations in the region

Stations	LCv	LCs	LCk	*D*
Bam	0.20	0.18	0.20	0.36
Birjand	0.11	0.09	0.21	1.11
Boujnord	0.21	0.03	0.15	3.02[a]
Chabahar	0.14	0.06	0.12	0.34
Isfahan	0.10	0.12	0.22	1.12
Fassa	0.20	0.13	0.08	1.16
Iranshahr	0.16	0.17	0.17	0.36
Kashan	0.18	0.22	0.22	0.05
Kerman	0.13	0.22	0.23	0.54
Khoor	0.32	0.70	0.66	5.45[a]
Sabzevar	0.12	0.07	0.08	0.35
Semnan	0.15	0.18	0.21	0.08
Shahrood	0.18	0.27	0.09	2.92
Shiraz	0.13	0.18	0.20	0.23
Tabbas	0.20	0.18	0.16	0.54
Torbat	0.15	0.12	0.13	0.12
Yazd	0.12	0.18	0.20	0.47
Zabol	0.15	0.14	0.19	0.13
Zahedan	0.12	0.21	0.18	0.68

[a]Shows discordant site.

To investigate the homogeneity of the region, the heterogeneity measure was used before and after removing discordant stations. The heterogeneity measure, H_1, for the region before and after removing discordant stations is 6.39 and 5.02, respectively. As the H_1 measure is greater than 2 for both before and after removing discordant stations, the region is considered heterogeneous. To find the homogeneous region based on the maximum annual wind speed in the arid and semi-arid regions of Iran, we begin a trial and error process.

In this process, the stations with the nearest L-moments to the weighted average L-moments are put into one group. The process repeats to get homogenous groups. In other words, the process continues until

homogeneity measure, H_1, is less than 1. The average weighted L-moments are shown in Figs. 2 and 3 with a "+" sign.

For the present study and after a trial and error process, a homogeneous region containing 10 stations among 17 stations (two stations were removed due to discordancy) was found. The homogeneity measure, H_1, for the selected region is 0.68, which shows the homogeneity of the region. Table 4 shows the L-moments and discordancy measures for the stations of the homogeneous region.

4.3. Identification of regional distribution model

The regional frequency distribution models for the homogeneous region are established on the basis of Z statistics (Eq. (11)). For this region, the qualifying distribution models (i.e., $|Z| < 1.65$) are shown in Table 5. In this table, it can be seen that Generalized Logistic (GLOG) distribution model is the best regional distribution model for both the entire region and the homogeneous region in comparison with other distribution models, Generalized Extreme values (GEV), three-parameter Log Normal (LN3), Pearson Type 3 (P3) and Generalized Pareto (GPAR) distribution models. The location, scale and shape parameters of the selected regional distribution (GLOG) model are 0.959, 0.135 and −0.177, respectively. Based on GLOG distribution as the regional distribution function, regional quantiles of the homogenous region are 28.02, 34.01, 38.22, 44.15, 49.15, 54.64 and 60.81 m/s for 2, 5, 10, 25, 50, 100 and 200-year return period, respectively. Although one can use these quantiles for any place "*within*" the homogeneous region, in the next section we develop a map based on at-site quantiles to give spatial variation of wind speed in the entire arid and semi-arid regions of Iran based on Kriging method.

4.4. At-site wind quantile estimation

Because the entire arid and semi-arid region of Iran is not homogeneous to apply one parent distribution for regional quantile estimation of the region, in this and the following sections, at-site wind speed quantile estimation is applied to create the regional map of annual maximum wind speed in different return periods for the entire region. The best at-site wind distribution model is selected based on the minimum root mean square

Table 4
L-moments and discordancy measures for the homogeneous region

Stations	LCv	LCs	LCk	D
Chabahar	0.13	0.04	0.07	1.70
Iranshahr	0.18	0.23	0.15	1.78
Kashan	0.18	0.22	0.20	1.47
Kerman	0.12	0.22	0.21	0.78
Semnan	0.14	0.18	0.19	0.41
Shiraz	0.13	0.17	0.18	0.24
Torbat	0.15	0.11	0.10	0.97
Yazd	0.11	0.18	0.17	0.58
Zabol	0.14	0.14	0.17	0.66
Zahedan	0.12	0.21	0.15	1.41

Table 5
Goodness-of-fit-test measures (Z^{Dist}) for study area

Region	GLOG	GEV	LN3	P3	GPAR
All stations	0.32[a]	−2.17	−2.48	−3.33	−7.63
Homogeneous region	−0.01[a]	−1.81	−2.06	−2.71	−5.78

[a]The distribution model is accepted as a regional distribution model.

error. Fig. 4 shows the cumulative distribution function fitted to each annual maximum wind speed series for each station. The wind quantiles for each station were then estimated by the use of maximum likelihood method and used for preparing the regional wind speed in different 10, 20, 50 and 100-year return periods.

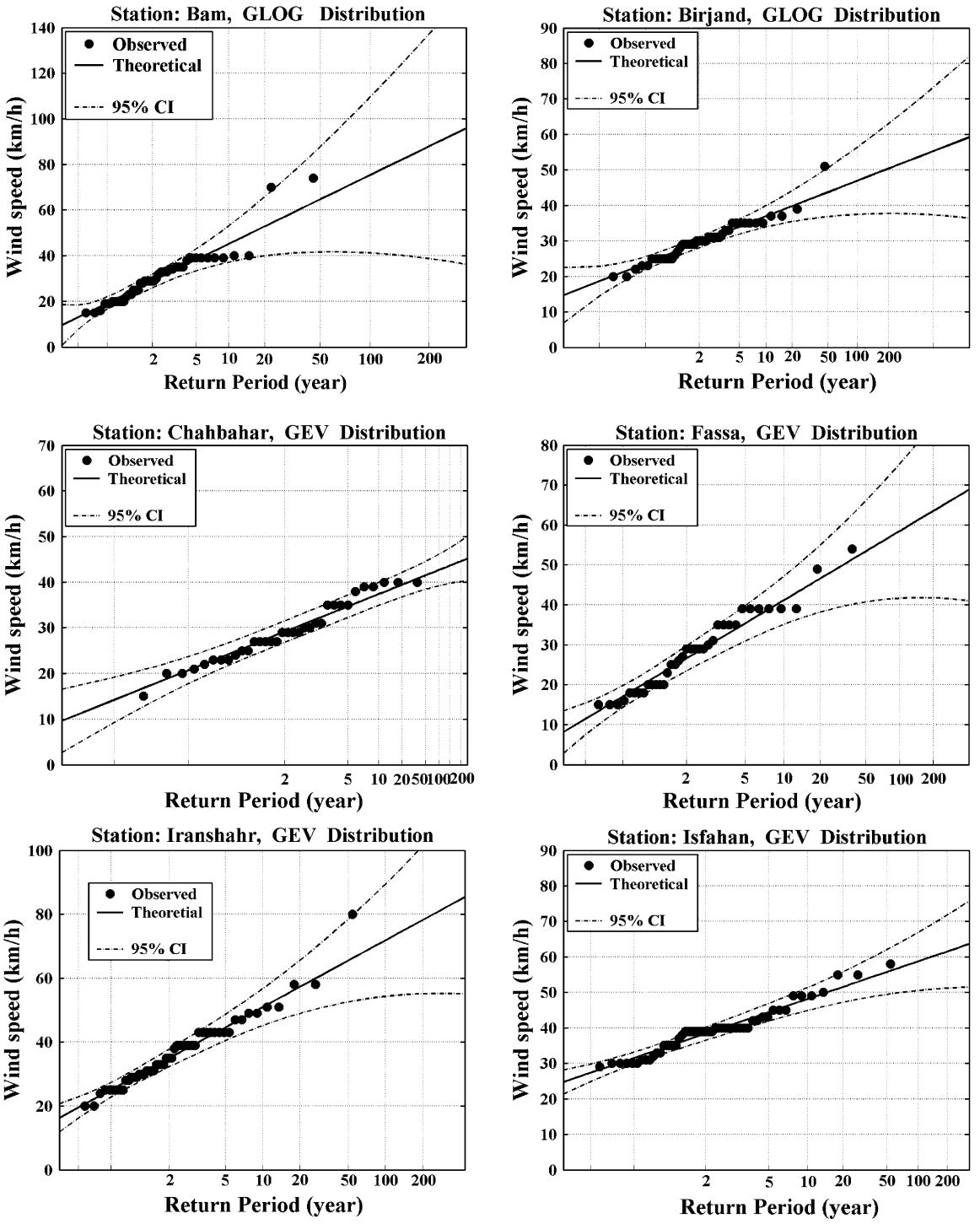

Fig. 4. Theoretical and observed probability plots of the annual maximum wind speed for arid and semi-arid region of Iran.

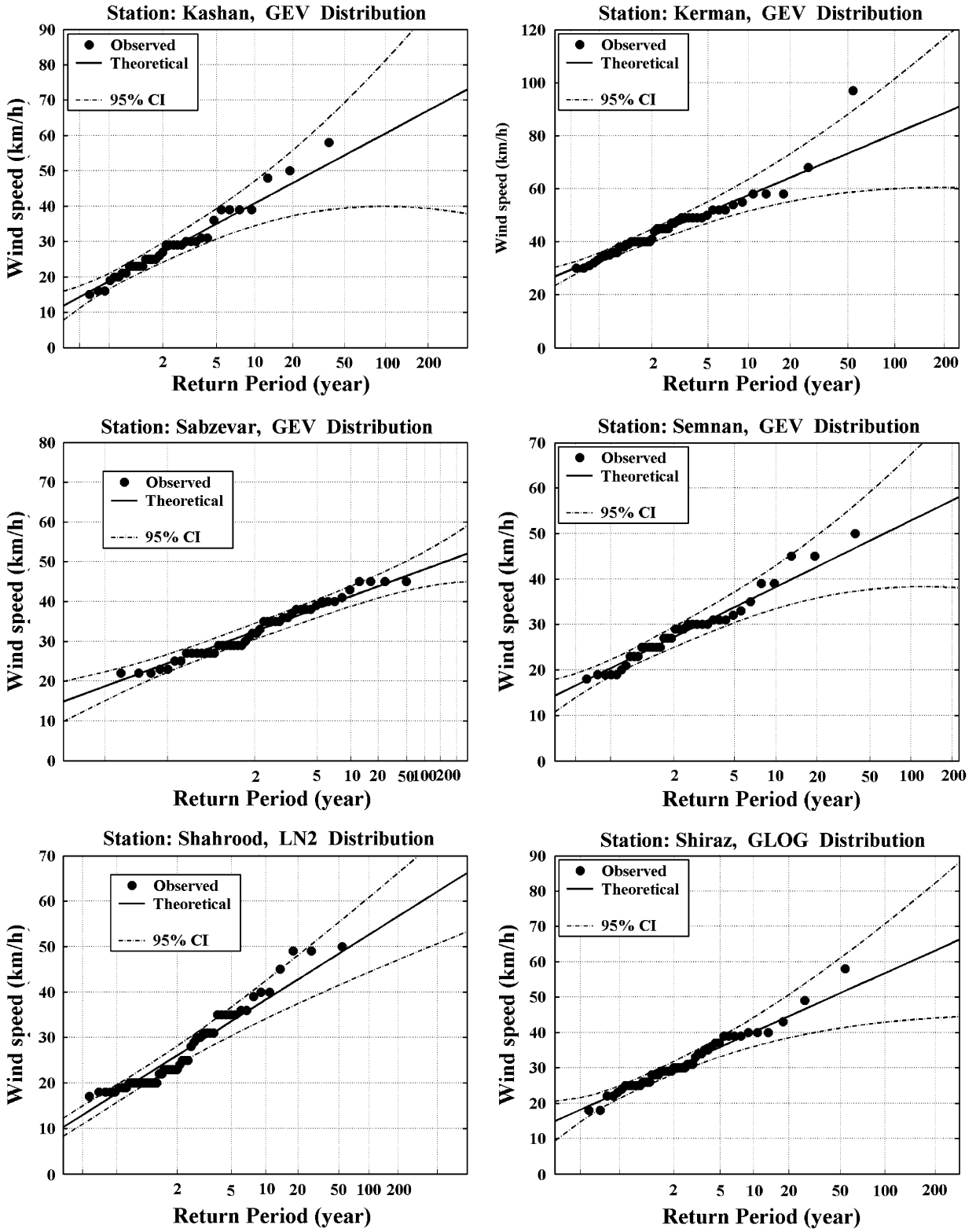

Fig. 4. (*Continued*)

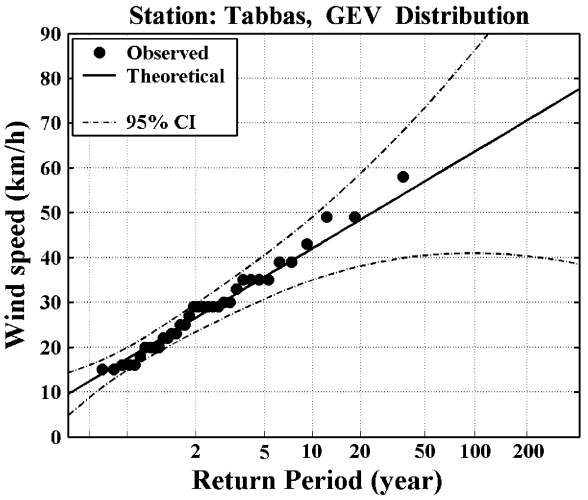

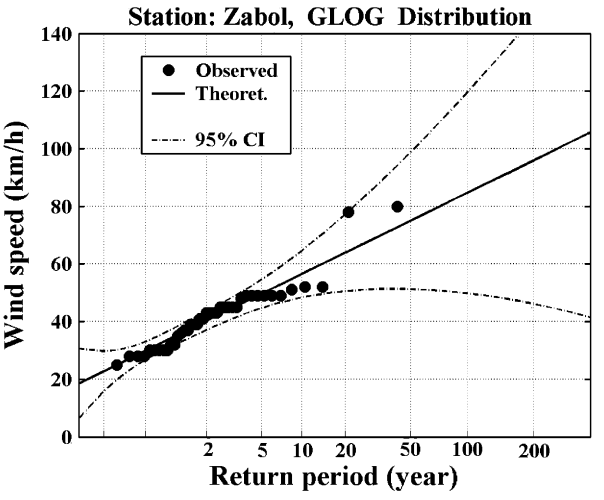

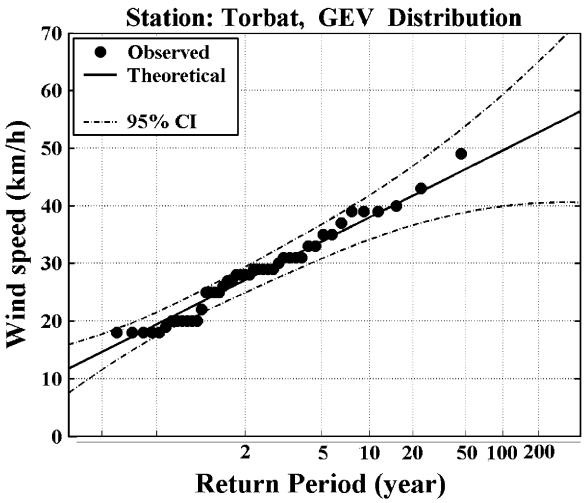

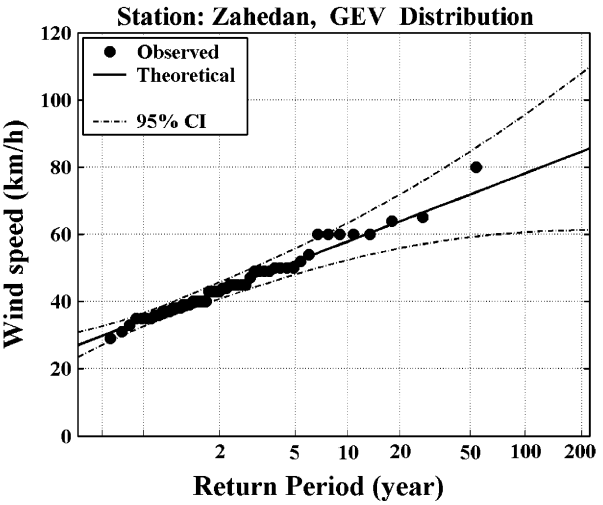

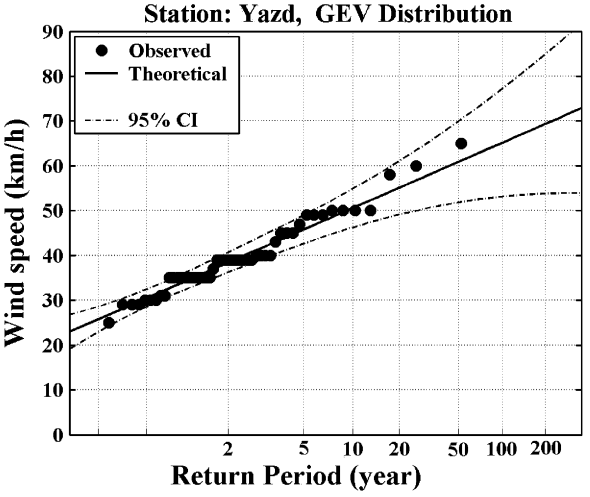

Fig. 4. (*Continued*)

For sites where no wind speed measurement is available, at-site quantiles were extended using the Kriging method to prepare a regional map of wind speeds variation in different return periods, 10, 20, 50 and 100-year return periods. Fig. 5 presents the regional wind speed curves for the study area.

From Fig. 4, it can be seen that the wind speed increases with the return periods. This implies that higher wind speed with higher erosive force occurs in longer periods with low probability as $Tr = 1/p$, where p is the probability of the wind speed. It is also obvious that wind speed increase rapidly in the center of the study area. Wind speeds are greatest in the north and southeast of the region.

4.5. Wind erosive power

In this section, we compare wind power of different return periods with 2-year return period wind speed. For standard atmosphere, where the average air density $\rho = 1.225\,kg/m^3$ at sea level and at temperature 15 °C, the instantaneous wind power density, WPD, in an air flow through a unit surface area perpendicular to the

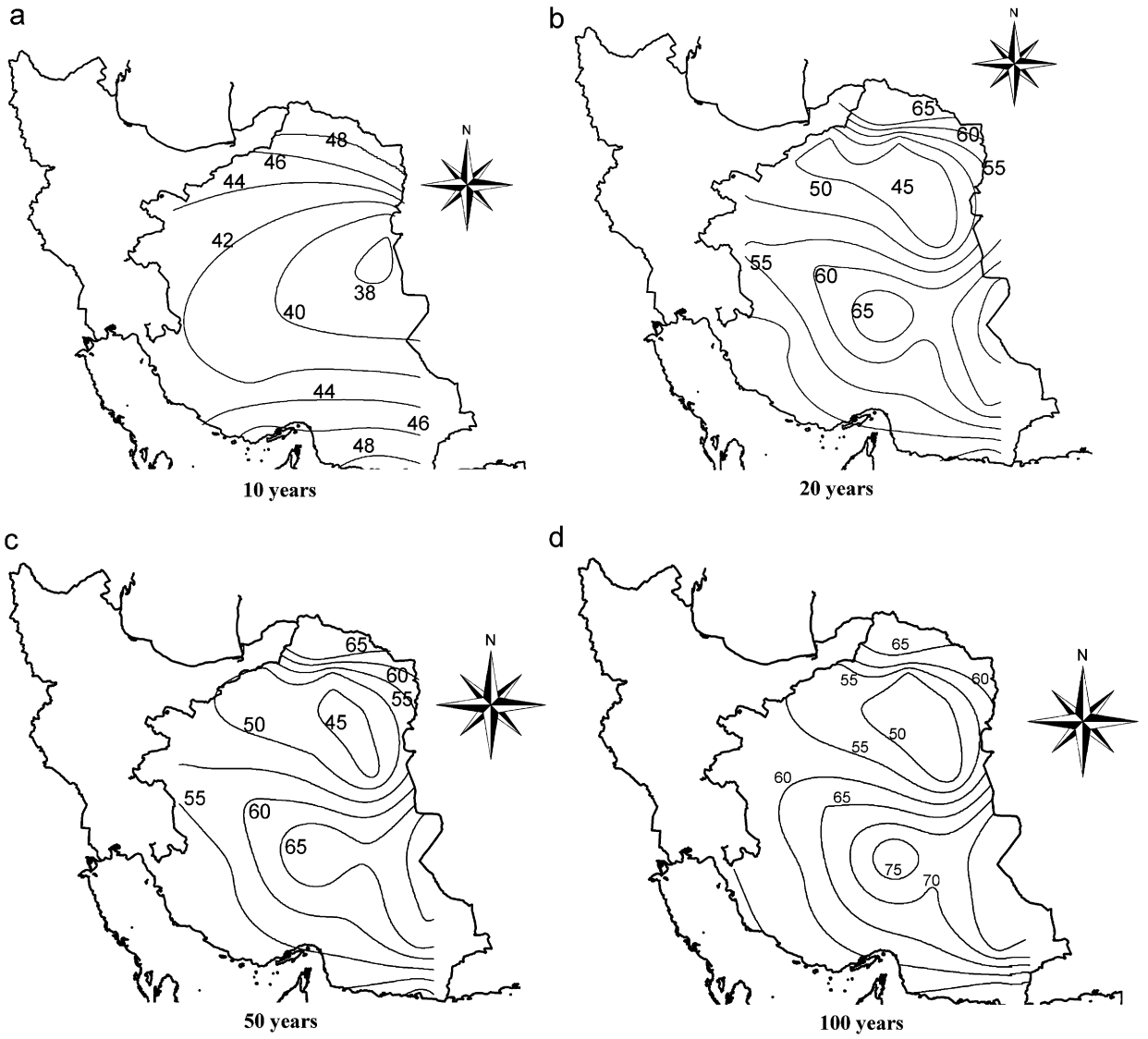

Fig. 5. Wind speed (km/h) of the arid and semi-arid region of Iran at different return periods (years): (a) Tr = 10, (b) Tr = 20, (c) Tr = 50, (d) Tr = 100.

Table 6
Wind energy ratio of different return periods (Tr) to 2-year return period wind

Station	Tr = 5	Tr = 10	Tr = 25	Tr = 50	Tr = 100	Tr = 200
Kashan	2.23	3.51	5.88	8.34	11.52	15.58
Kerman	1.77	2.52	3.86	5.22	6.97	9.21
Semnan	1.92	2.79	4.27	5.67	7.37	9.41
Shiraz	1.72	2.40	3.64	4.97	6.81	9.36
Yazd	1.69	2.28	3.18	3.98	4.87	5.88
Zahedan	1.73	2.40	3.53	4.60	5.92	7.52
Zabol	1.87	2.76	4.49	6.46	9.32	13.50
Iranshah	2.21	3.55	6.23	9.22	13.40	19.36
Chahbaha	1.68	2.10	2.58	2.88	3.13	3.34
Torbat	1.94	2.75	3.97	5.01	6.15	7.38
Bam	2.24	3.54	6.15	9.13	13.46	19.72
Birjand	1.52	1.92	2.55	3.12	3.80	4.62
Boujnord	2.31	3.28	4.48	5.30	6.04	6.70
Isfahan	1.55	1.97	2.57	3.06	3.58	4.12
Fassa	2.36	3.70	5.97	8.11	10.66	13.63
Khoor	2.83	4.81	8.42	12.03	16.52	21.97
Sabzevar	1.64	2.06	2.58	2.94	3.26	3.56
Shahrood	2.55	3.19	4.88	6.43	8.23	10.31
Tabbas	2.22	3.14	4.37	5.31	6.26	7.23
Mean	2.00	2.88	4.40	5.88	7.75	10.13
Maximum	2.83	4.81	8.42	12.03	16.52	21.97

air stream during a unit time is derived classically as

$$\mathrm{WPD} = \tfrac{1}{2}\rho V^3,$$

where V is the wind speed and the unit of WPD is W/m^2 provided that V is in m/s. In the derivation, one of the basic assumptions is that the air density is constant at its average level, wind speed is the instantaneous value and hence, it is implied that they are independent from each other (Sen, 2000).

Thus, if all conditions are assumed to be equal, the wind erosive energy is related to the cubed value of wind speed. Table 6 shows the ratio of wind energy of different return period to annual wind speed. The mean of the ratios varies from 2 to 10.13 from 5 to 200-year return period. The maximum values can be seen for Khoor station, located at the center of arid region of Iran, while the minimum values belong to Birjand station, located in northwest of arid region of Iran.

It can be seen that the erosive power ratio increases with nonlinear trend while the return periods increase. For example, the wind energy of a 5-year return period wind speed is 2.23 times higher than that of a 2-year return period at Kashan station. Another example is the ratio of the 200-year return period wind speed at Khoor station, which is 22 times higher than the 2-year return period speed.

Within the homogeneous region, Iranshahr, Kashan and Zabol have the highest ratios, which are located in southeastern, center and southeastern parts of the arid and semi-arid region of Iran, respectively.

5. Conclusions

Wind erosion control and management is an essential task in arid and semi-arid region. Managers and wind erosion structure designers need to know the risk of erosive wind in a region. In addition to the analysis of the impacts of wind erosion for risk analysis, the frequency or the probability of the occurrence of erosive wind speeds is also important. To assess the regional probability or return period of annual maximum wind speeds in the arid and semi-arid regions of Iran, we applied regional frequency method of L-moments. The results showed that GLOG distribution model is the best regional frequency analysis for wind homogeneous region derived from homogeneity measures. This study also prepares the regional annual maximum wind speed map for the arid and semi-arid region of Iran in different return periods. These regional curves showed that wind

speed is higher in the center, northwest and southwest of the region in different return periods. Although wind erosion does not depend on wind speed only, but wind speed frequency analysis will help wind erosion managers to find vulnerable areas to wind erosion and extend at-site results to larger areas with no available data. The comparison of wind energy for different return periods showed that the wind erosive energy increases with a nonlinear trend as the return periods increase. This indicates the importance of wind frequency analysis in wind erosion control and management. In other words, a manager should pay enough attention to the risk (probability) of the occurrence of erosive winds in the period of design life of the structures and facilities of wind erosion control as the wind force increases nonlinearly in higher return periods. In general, it is strongly recommended to take into account the wind frequency analysis, both at site and regional, for wind erosion management and control projects.

References

Cornelis, W.M., Gabriels, D., 2005. Optimal windbreak design for wind-erosion control. Journal of Arid Environment 61, 315–332.

Cunderlik, J.M., Burn, D.H., 2002. The use of flood regime information in regional flood frequency analysis. Hydrological Sciences Journal 47, 77–92.

Goel, N.K., Burn, D.H., Pandey, M.D., An, Y., 2004. Wind quantile estimation using a pooled frequency analysis approach. Journal of Wind Engineering and Industrial Aerodynamics 92, 509–528.

Gomes, L., Arrué, J.L., López, M.V., Sterk, G., Richard, D., Gracia, R., Sabre., M., Gaudichet, A., Frangi, J.P., 2003. Wind erosion in a semiarid agricultural area of Spain: the WELSONS project. Catena 52, 235–256.

Greenwood, J.A., Landwahr, J.M., Matalas, N.C., Wallis, J.R., 1979. Probability weighted moments: definition and relation to parameters of several distribution models expressible in inverse form. Water Resources Research 15 (5), 1049–1054.

Hosking, J.R.M., 1990. L-moments: analysis and estimation of distribution using linear combination of order statistics. Journal of the Royal Statistical Society B 52, 105–124.

Hosking, J.R.M., Wallis, J.R., 1993. Some statistics useful in regional flood frequency analysis. Water Resources Research 23, 271–281.

Lopez, M.V., 1998. Wind erosion in agricultural soil: an example of limited supply of particles available for erosion. Catena 33, 17–28.

Okin, G.S., Murray, B., Schlesinger, W.H., 2001. Degradation of sandy arid shrub-land environments: observations, process modeling, and management implications. Journal of Arid Environments 47, 123–144.

Reed, D.W., Jacob, D., Robson, A.J., Faulkner, D.S., Stewart, E.J., 1999. Regional frequency analysis: a new vocabulary. In: Gottschalk, L., Olivry, J.-C., Reed, R. (Eds.), Hydrological Extremes: Understanding, Predicting, Mitigating, Proceedings of the Birmingham Symposium, July 1999, No. 255. IAHS Publication, pp. 237–243.

Sen, Z., 2000. Stochastic wind energy calculation formulation. Journal of Wind Engineering and Industrial Aerodynamics 84, 227–234.

Song, Z., 2004. A numerical simulation of dust storms in China. Environmental Modeling and Software 19, 141–151.

Stedinger, J.R., Vogel, R.M., Foufoula-Georgiou, E., 1993. Frequency analysis of extreme events. In: Maidment, D.R. (Ed.), Hand Book of Hydrology. McGraw-Hill, New York, pp. 18.1–18.66.

Stout, J.E., Lee, J.A., 2003. Indirect evidence of wind erosion trends on the Southern High Plains of North America. Journal of Arid Environment 55, 43–61.

Vogel, R.M., Fennessey, N.M., 1993. L-moment diagram should replace product moment diagram. Water Resources Research 29 (6), 1745–1752.

WEPS, 1996. Wind erosion prediction system. Kansas State University, URL page: 〈http://weru.ksu.edu〉.

Zobeck, T.M., van Pelt, R.S., 2006. Wind-induced dust generation and transport mechanics on a bare agricultural field. Journal of Hazardous Materials 132, 26–38.